The Laboratory Spectroscopy of True Molecular Line Shape in MM/SubMM Range under Pressures from 0.1 to 1000 Torr

M.Yu. Tretyakov*
Institute of Applied Physics of RAS, 46 Uljanova Str. 603950, Nizhny Novgorod, Russia

ABSTRACT

The review of modern methods of precision measurements of spectral line parameters used in Microwave Molecular Spectroscopy Laboratory in Nizhny Novgorod is presented. Various line shape models used for measurements of spectral line parameters are considered. Analysis of possible sources of systematic errors in parameters determination is given. Wide-range spectral studies possibilities and high accuracy of obtained parameters are demonstrated on example of investigations of practically important for atmosphere remote sensing spectral lines of water and oxygen by means of two spectrometers with complementary abilities.

Keywords: Molecular spectroscopy, line shape, precision measurements, millimeter and submillimeter waves, high resolution, atmospheric lines.

1. INTRODUCTION

Millimeter- and submillimeter-wave range is a range of rotational spectra of majority of light molecules. This universality of the range makes it very attractive for molecular analysis and in particular for remote sensing of planetary atmospheres and interstellar space researches, so the number of satellites utilizing the millimeter- and submillimeter-wave instruments is rising up every year (see e.g. recent review [1]). Laboratory spectroscopy provides important information for such kind of researches. Nowadays, in addition to traditional line center frequencies and peak intensities, precise knowledge of other spectral line properties such as pressure broadening, pressure shifting of the line center including broadening and shifting by foreign gases, line mixing, and their temperature dependencies are demanded. These data are rare in spectroscopic databases, and even for most common molecular lines experimental values of these parameters often are not known. Better knowledge than traditional 30 kHz databases accuracy of spectral lines central frequencies is also demanded e.g. by astrophysicists for analysis of space molecular clouds movement using Doppler effect [2]. Also cases when parameters measured in some papers differ much more than errors quoted by authors are quite common. Evident cause of lesser abundance of precise data is difficulty of accurate measurements of line parameters, therefore analysis and improvement of methodics of these measurements are essential.

The paper deals with precision measurement of spectroscopic parameters, which can be extracted from the shape of observed molecular lines. Two spectrometers in their modern versions are described. Both spectrometers are based on MM/SubMM backward-wave oscillator (BWO) tubes phase-locked against harmonic of frequency standard. The first one is automated spectrometer with acoustical detection (RAD) of radiation absorption operating in pressure range from hundreds of milliTorr to ten Torr [3]. The second one is the resonator spectrometer with fast digital back and forth frequency scanning operating in a pressure range up to atmosphere [4]. Use of various line shape models for experimentally observed collision-broadened lines in mm/submm wavelength range is demonstrated. Sources of line parameters determination errors such as wrong line shape model selection, improper accounting for baseline or apparatus function, limiting range of line record are analyzed. Less than 10 kHz measurement accuracy of rather weak oxygen lines central frequencies and 10 kHz/Torr accuracy of the line pressure broadening parameters determination, ~1% measurement accuracy of 183-GHz water line integral intensity, first experimental measurement of a small mixing parameter for 118 GHz oxygen line achieved in our experiments as result of treatment of observed with high signal-to-noise (S/N) ratio shapes of spectral lines and careful accounting for the line shape distortion factors.

* trt@appl.sci-nnov.ru; phone: 7-8312-16-48-66; fax: 7-8312-36-37-92; http://appl.sci-nnov.ru/mwl/

14th Symposium on High-Resolution Molecular Spectroscopy,
edited by Leonid N. Sinitsa, Proceedings of SPIE Vol. 5311 (SPIE,
Bellingham, WA, 2004) · 0277-786X/04/$15 · doi: 10.1117/12.545191

2. THEORETICAL ANALYSIS

2.1 Common definitions and assumptions

The transmission of monochromatic radiation through homogeneous gas sample is described by Beer-Lambert law:

$$I(\nu) = I_0(\nu) \cdot e^{-\alpha(\nu)L}, \tag{1}$$

where I_0 and I are correspondingly the radiation incident and transmitted intensities both as functions of the radiation frequency ν; L – the absorption path length, and $\alpha(\nu)$ – the gas absorption coefficient which can be expressed as:

$$\alpha(\nu) = \alpha_{\text{int}} \cdot F(\nu),$$

where $F(\nu)$ – is normalized line profile and α_{int} – is integrated absorption coefficient of individual molecular spectral line:

$$\alpha_{\text{int}} = \int_{line} \alpha(\nu) d\nu \qquad \text{and} \qquad \int_{line} F(\nu) d\nu = 1 \ .$$

The line intensity (α_{line}), which is in fact the value presented in spectroscopic databases, is usually defined as: $\alpha_{line} = \alpha_{\text{int}} / N$, where N is density of absorbing molecules. It should be noted that α_{line} can be calculated for any particular line and it has multiplicative frequency dependent terms, what is important for the experimental line shape analysis especially in the case of broad atmospheric lines.

Choice of particular line profile $F(\nu)$ depends on conditions of experiment. If the collisional broadening is negligibly small and only Doppler effect determines the line broadening, then the Gauss (or Doppler) profile can be used:

$$F_D(\nu) = \frac{1}{\gamma_D} \cdot \sqrt{\frac{\ln 2}{\pi}} \cdot e^{-\ln 2 \cdot \left(\frac{\nu - \nu_0}{\gamma_D}\right)^2},$$

where ν_0 – is the line central frequency and γ_D – is the Doppler half width at half maximum (HWHM). In the case of free-space static pressure gas cell it can be calculated as:

$$\gamma_D = \frac{\nu}{c} \sqrt{2 \cdot \ln 2 \cdot \frac{kT}{M}},$$

where c – is the speed of light, k – the Boltzmann constant, T – temperature and M – the molecular weight of absorbing gas in atomic mass units.

If the Doppler line width is negligibly small and the line broadening results from collision but still the line width is much less than the line central frequency, then the Lorentz line-shape function is used:

$$F_L(\nu) = \frac{1}{\pi} \cdot \frac{\gamma_L}{(\nu - \nu_0)^2 + \gamma_L^{\,2}},$$

where γ_L – is the Lorentz line HWHM.

For broad collisional lines the Van Vleck-Weisskopf line-shape is more appropriate:

$$F_{VVW}(\nu)=\frac{\nu}{\pi\cdot\nu_0}\cdot\left(\frac{\gamma_L}{(\nu-\nu_0)^2+\gamma_L{}^2}+\frac{\gamma_L}{(\nu+\nu_0)^2+\gamma_L{}^2}\right).$$

In the intermediate pressure range between pure Doppler and pure Lorentz broadening the Voigt profile is used, obtained in assumption that each collision is unable to perturb the Maxwell distribution of molecular velocities or in other words that there is no correlation between collisions and velocity distribution as a convolution of aforementioned $F_D(\nu)$ and $F_L(\nu)$ profiles:

$$F_V(\nu)=F_D(\nu)\otimes F_L(\nu)=\int_{-\infty}^{\infty}F_D(t)F_L(\nu-t)dt=\frac{y}{\pi\cdot\gamma_D}\cdot\sqrt{\frac{\ln 2}{\pi}}\cdot\int_{-\infty}^{\infty}\frac{\exp(-t^2)}{(x-t)^2+y^2}dt,$$

where

$$x=\frac{\nu-\nu_0}{\gamma_D}\cdot\sqrt{\ln 2},\qquad y=\frac{\gamma_L}{\gamma_D}\cdot\sqrt{\ln 2}.$$

These four classical models correspond to experimentally observed shapes of spectral lines to the better than one percent accuracy in a practically informative (i.e. about 10-15 linewidths) vicinity of the line center for majority of experimental studies. A systematic discrepancies between the experimental and calculated profiles can rise up to a few percents or more in a few following cases:

i) The discrepancies between the experimental and calculated Voigt profiles of the order of a few percents occur when the Doppler width is at least comparable with the Lorentz width and become more essential when the Doppler broadening contributes significantly (e.g. [5]). The observed line width is less than expected (Dicke collisional narrowing effect). That kind of discrepancies can be removed by one of the following methods either using models including the reduction of Doppler broadening due to effect of velocity changing collisions: a) Rautian-Sobel'man model [6] – uncorrelated hard collisions (best suited when the perturber mass is larger than the radiator one); b) Galatry model [7] – uncorrelated soft collisions (best suited when the active molecule mass is lager than the perturber one); or introducing speed dependence of collisional relaxation rate: c) Speed Dependent Voigt model [8]. In all aforementioned cases the discrepancy is removed by the cost of one more adjustable constant. It should be mentioned, that this kind of discrepancy formally can be removed simply by using the Dopper width as adjustable parameter in the Voigt model (e.g. [9]).

ii) In the case of rather high molecular density (pressure range of about 100 Torr and higher) in the spectral range of line clusters (like dense Q-branches etc.) the discrepancy between observed spectrum and absorption calculated as a simple sum of Lorentz or Van Vleck-Weisskopf profiles can reach up to tens percents. The effect is known as line mixing (blending, interference etc.). A simple model accounting for the effect in a first order approximation was developed by P. Rosenkranz [10]. The model employs one more parameter called mixing coefficient and it is roughly equivalent to Lorentz function multiplied by linear with frequency term. The model is sufficiently accurate for the most atmospheric applications.

iii) Range of far line wings is still quite a vague area (classical example is water molecule). For practical applications semi-empirical models are used.

2.2 Experimental factors affecting the shape of observed spectral line

Let us consider shortly a few most principal factors affecting observed line shape in experimental studies:

2.2.1

Amplitude-frequency dependence of radiation interacting with molecules, including radiation interference in the spectrometer wave-guides and power-frequency properties of the radiation source and detector. This factor plays essential role in majority of spectroscopic experiments including even observation of narrow Doppler broadened lines. The factor is in fact taken into account in equation (1) by frequency dependence of incident power. In many practical

cases of narrow lines usually associated with high-resolution molecular spectroscopy the frequency dependence of $I_0(\nu)$ in the line center vicinity can be sufficiently well approximated by second or even first order polynomial.

2.2.2 Spectral width of the spectrometer radiation source.
If the width is not negligible as compared with width of a spectral line then the observed signal can be expressed as a convolution of molecular absorption signal with spectral function of the source $Sp(\nu)$, so following equation should be used instead of equation (1):

$$I(\nu) = I_0(\nu) \cdot e^{-\alpha(\nu)L} \otimes Sp(\nu).$$

2.2.3
Line broadening effect due to molecular collisions with walls of gas cell of spectrometer and (2.2.4) power saturation effect which occur when number of photons absorbed by molecules per time unit is comparable or bigger than number of collisions. The best way to take these both effects into account is a careful choice of experimental conditions so the effects influence is negligible.

It should be also noted that to get the best shapes of molecular lines one should carefully take care about minimization of variation of various spectrometer parameters either mechanical or electrical that is usually related to a temperature drift.

The factors listed above are quite known and the most important part for precision measurement is how to take them into account so they do not limit high accuracy of experimental measurements.

2.3 Possible problems with spectral line parameters determination
Parameters of spectral line are determined as results of the best fit of theoretical lineshape model to experimentally observed profile. Statistical accuracy of the parameters determination directly depends on the observed profile S/N ratio. Apart from that there are other factors leading to systematical error of the parameters, what in some cases considerably exceed statistical errors. Let us demonstrate by means of computer experiment a few most common cases:

2.3.1 Improper line shape model selection.
It's quite difficult to decide which particular model has to be used for some particular experiments especially in the border range of models. For instance, if the Lorentz function is sufficiently good when the collisional width is an about order of magnitude bigger than Doppler width or Voigt model should be used still? Let's compare these two models on example of isolated water line at 183 GHz broadened by air (broadening parameter 3.84 MHz/Torr @ 298K [20]). Left plot in Fig. 1 presents the shape of the water line in air with amplitude normalized to unity, calculated for room temperature and air pressure of 0.5 Torr ($\gamma_L/\gamma_D \sim 7.1$) within 15 line halfwidths using known line parameters and Voigt model (curve "*A*"). The curve simulates experimental record of the line. The same figure presents Lorentz function as a theoretical model fitted to the "experimental" Voigt curve. The two curves coincide to the thickness of the line (curve "*A*"). Their difference expanded by factor of 10 is shown below by curve "*B*". As it's seen from the figure the difference can be observed only if experimental S/N ratio is bigger than ~300, which is quite a good ratio for a real experiment. For clarity the curve "*C*" demonstrates the difference (also expanded by factor of 10) between the Voigt and Lorentz curves in the case when random data with normal distribution and standard deviation 0.0033 was added to the Voigt curve simulating an experimental noise. Thus the noise-looking residual demonstrates apparent adequacy of the fitting model. The line width is determined from the fit with statistical accuracy (one standard deviation) of about 0.15% but it's absolute deviation from the true width (in other word the systematical error of the "experiment" is 1.4%, i.e. almost 10 times bigger than statistical error.

Similar calculations demonstrate that use of the Lorentz lineshape model for the same 183-GHz water line in air record (see plot on the right in Fig.1) simulated for near atmospheric pressure 635 mmHg ($\gamma_L/\nu_0 \sim 0.013$, S/N ~ 300) instead of the Van Vleck-Weisskopf model (the models are also undistinguishable within experimental accuracy as it's seen from the noise-looking residual) does not give systematic error in the line width determination, but does give the systematic error of the line central frequency exceeding the standard deviation of the parameter determination by order of magnitude. In other words the experiment shows apparent negative frequency shift of the line center of about 30 MHz.

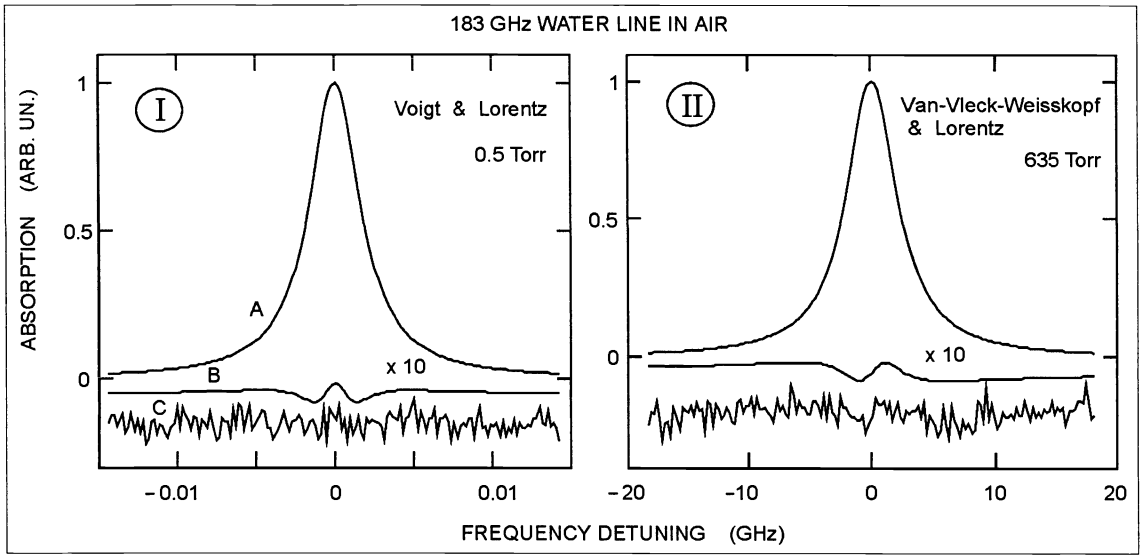

Fig. 1. Simulated records of 183 GHz water line in air at room temperature and result of their fitting to Lorentz line shape model: (A) Pressure 0.5 Torr. Voigt profile was used for the simulation; (B) 635 Torr, Van Vleck-Weisskopf profile was used for the simulation. Ten times enlarged residuals of the fit are shown below (see text for the explanation).

2.3.2 Improper accounting for baseline or apparatus function

It's common practice to consider the spectrometer apparatus function by multiplicative term in the lineshape model. However, spectrometers very often may also produce signals equivalent to additive molecular absorption e.g. absorption by a gas cell walls. To analyze possible consequences we fitted simulated record (S/N ~ 300, record range $15\gamma_L$) of the same 183-GHz water line in air under pressure 1 Torr having additive frequency dependent components to the Lorentz model function with multiplicative frequency dependent terms only. The criterion of analysis again was the noise looking fit residual i.e. undistinguishable models. The analysis showed that if the line record had only linear with frequency additive term then the γ_L parameter can be determined without systematical error but the line center ν_0 had systematical shift of the order of 50 kHz exceeding the statistical error of the parameter determination (one standard deviation) in about order of magnitude. On the contrary, the quadratic with frequency additive term lead to about 1% systematic error of the γ_L parameter determination also exceeding statistical error in order of magnitude. Similar problems occur in case of attempts to describe multiplicative apparatus functions by additive terms to fitting function.

2.3.3 Limiting range of the line record

Influence of this factor becomes essential if improper model is chosen for the experiment data fitting. The influence occurs due to correlation of fitting parameters (e.g. the line width and the baseline terms). For example, broadening of the Voigt profile can be partly compensated by quadratic with frequency additive term to the Lorentz model keeping apparent sufficiency of the Lorentz model but increasing systematical error of the line width determination. In particular, measured width of the aforementioned simulated record of 183-GHz water line in air at 0.5 Torr pressure has systematical error 1.6% if the record range is $20\gamma_L$ and 3.5% if the range is $3\gamma_L$. In general, wider range of an experimental record helps for better understanding of an apparatus function of used spectrometer.

As an example of possible systematic experimental errors Fig. 2 presents graphical review of the 183-GHz water line broadening by air parameter measurement results obtained by different authors using different experimental methods. Difference in the parameter values constitutes more than 20% and in some cases exceeds an experimental uncertainty given by authors in a few times. Our results (points number 11 [4] and 12 [20]) being somewhere in the middle of other values have better estimated accuracy. Nevertheless, the use of the calculated apparatus function in work [4] (point 11) introduced a small systematic error exceeding the estimated accuracy, so the value is a bit higher than more precise value from our later work [20] (point 12), where the apparatus function was measured experimentally so its influence was minimized.

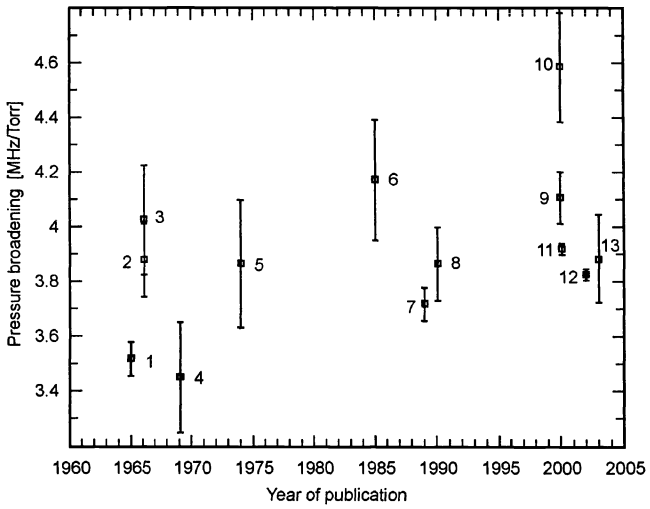

Fig. 2. Measured values of the water line pressure broadening parameter (recalculated to T=300K). The authors responsible are as follows. 1: Rusk [11], 2: Dryagin et al. [12], 3: Frenkel and Woods [13], 4: Hemmi and Straiton [14], 5: Ryadov and Furashov [15], 6: Bauer et al. [16], 7: Bauer et al. [17], 8: Goyette and DeLucia [18], 9: Pumphrey and Buehler [19] – MLS, 10: Pumphrey and Buehler [19] – MAS, 11: Krupnov et al. [4], 12: Tretyakov et al. [20], 13: Toth and Brown [21]. (Bulk data for the picture are taken from [19].)

3. EXPERIMENTAL EXAMPLES

3.1 Line-shape spectroscopy with RAD spectrometer

Block-diagram of RAD spectrometer is presented in Fig. 3. The radiation source of the spectrometer is BWO stabilized by phase locking of its radiation frequency against harmonic of millimeter-wave range synthesizer. The synthesizer in its turn employs a signal from Rubidium standard as a frequency reference. The absorption cell of RAD spectrometer is equipped with a highly sensitive microphone. A resonance absorption by the gas of the chopped BWO radiation induces a periodic temperature/pressure variation (acoustic signal) inside the cell, which is registered by the microphone. The spectrometer employs digital synchronous detection of the signal. The radiation frequency setting and data acquisition are controlled by computer.

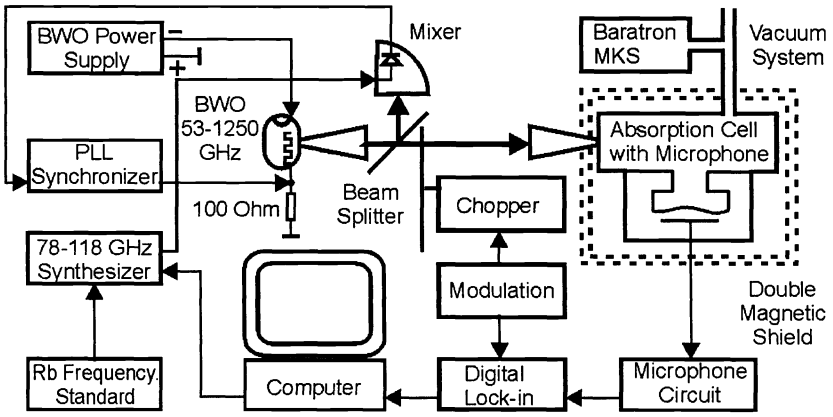

Fig. 3. Block-diagram of RAD spectrometer.

It was shown earlier in our works that the spectrometer is very well suited for study of line pressure shifting and broadening because of its principle of absorption signal detection. In opposition to conventional video-spectrometers where the useful signal is observed in the presence of a large uninformative background, the output signal in RAD spectrometer appears only if there is radiation absorption inside the cell. Some shortcomings still persist although to a lesser extent. Let's analyze here some possible sources of RAD spectrometer observed line shape distortion. The

stabilized radiation source in the spectrometer has a spectrum bandwidth of about few kHz, which is at least in three orders of magnitude less than usual width of observed lines, so its influence on observed shapes of molecular lines can be neglected. The spectrometer output signal S is related to the power loss (I_0–I) in the gas cell, and can be expressed from eq. (1) as:

$$S = I_0(\nu)\cdot\alpha(\nu)\cdot L \qquad (\text{for } \alpha(\nu)\cdot L << 1).$$

This approximation is valid for the most lines since the cell length is only 10 cm. Of course, if necessary full exponential expression can be used. Thus the spectrometer sensitivity is in direct proportion to radiation power I_0 (which is, by the way, another big advantage of the spectrometer). So amplitude-frequency characteristic of the radiation source and radiation interference in spectrometer wave-guide parts should be taken into account as a multiplicative term to the line shape function. Moreover relatively high power of BWOs (up to 100 mW) used in some experiments lead to appearance of rather weak but yet noticeable parasitic signals coming from absorption of the radiation in the RAD gas cell windows as well as in elements of microphone. The value of the signal also depends on the incident power I_0, and appears as additional absorption signal. It was found that for majority of observed lines in the pressure range up to a few Torrs a combination of constant- and linear-with-frequency multiplicative terms and constant-, linear- and sometimes quadratic with-frequency additive terms are sufficient to account for both aforementioned distortions. Thus, the total line shape function to be used for fitting to RAD spectrometer experimental data should look like:

$$S_{RAD}(\nu) = A_0\cdot(1+A_1(\nu-\nu_0))\cdot F(\nu)+A_2+A_3(\nu-\nu_0)+A_4(\nu-\nu_0)^2, \qquad (2)$$

where A_i are adjustable coefficients. The most practical lineshape models for $F(\nu)$ in a pressure range of RAD experiments are the Lorentz and Voigt profiles.

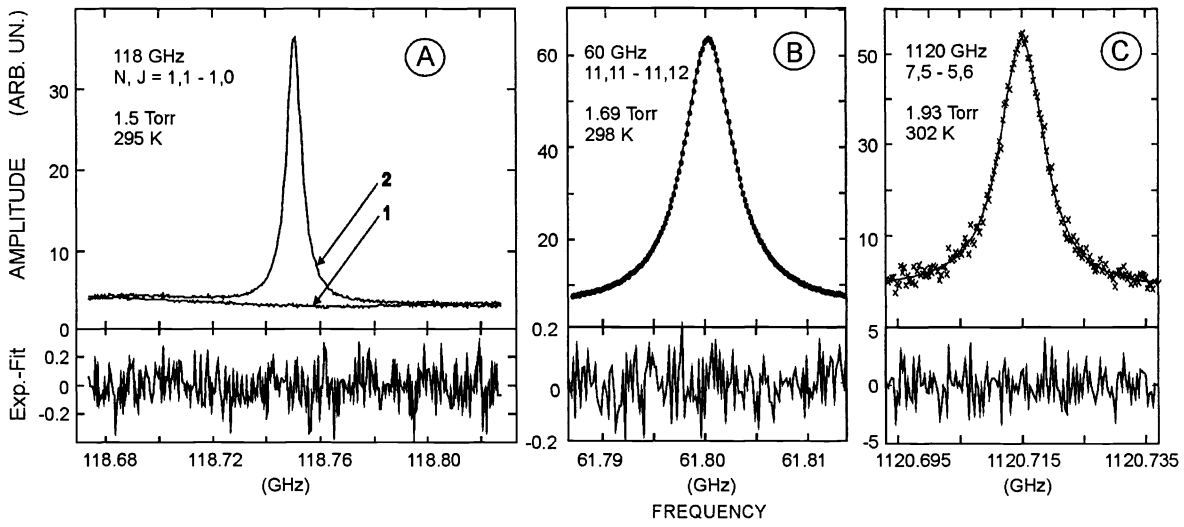

Fig. 4. Examples of oxygen spectral lines recorded with RAD spectrometer and result of their fit to model function. Identification of transitions in form of $N',J' - N,J$ as well as experimental pressure and temperature are shown in the figures. (A) 118-GHz line in pure oxygen (trace 2) and the apparatus function (trace 2) recorded with the cell filled by non-absorbing gas (pure nitrogen) at the same pressure 1.50 Torr. Lower part of the figure presents residual of the fit of the Lorentz model with multiplicative linear with frequency term to difference of traces 2 and 1. (B) One of 60-GHz oxygen band lines. (C) 1.12 Terahertz oxygen line.

The use of the function (2) gives sufficiently good results for most experimental records with the spectrometer. Although in some difficult cases it was found practical to fill the spectrometer cell with non-absorbing gas under the same pressure as the studied sample and to subtract the apparatus function obtained in this way from the line record as shown in Fig. 4A. The upper part of the figure is a record of the 118-GHz line in pure oxygen (trace 2) and signal from the cell when the oxygen was replaced by pure nitrogen under the same pressure (trace 1). The lower part of the figure presents residual of the fit of function (2) (having only multiplicative term to $F(\nu)$) to the difference of traces 2 and 1 assuming the Lorentz model. The figure demonstrates good S/N ratio (about 300) of the observed line. The noise-like residual

demonstrates adequacy of the fitted line shape function to the experimental data. The procedure allows to get rid from the aforementioned additive terms in the fitting function and thus to reduce number of fitting constants.

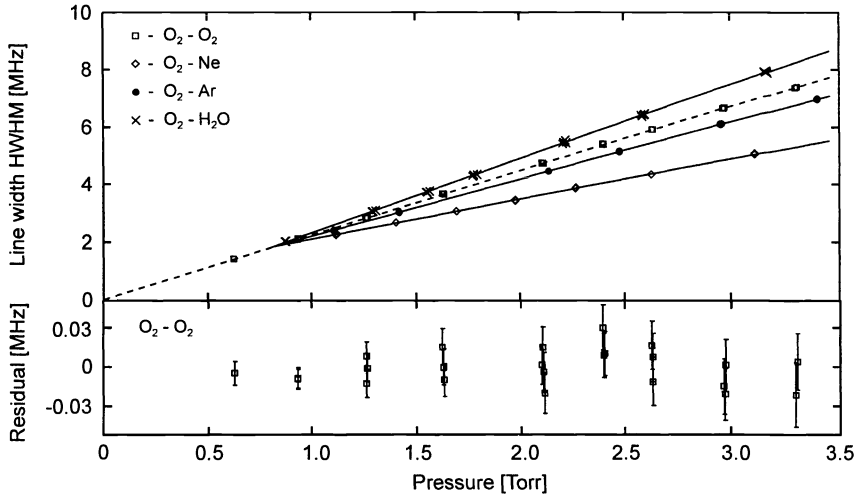

Fig 5. Broadening of 118 GHz oxygen line by pressure of various atmospheric species measured by use of RAD spectrometer at room temperature. For all experiments except self-broadening the partial pressure of oxygen was kept near 0.8 Torr. Designation of experimental points is shown in the picture. The lines correspond to the best fit of linear function to experimental points. The self-broadening experiment is emphasized by dashed line. The residual of the fit of self-broadening points is shown below in expanded scale.

Results of the study of the 118-GHz oxygen line broadening by various atmospheric species using the RAD spectrometer [22] are presented in Fig. 5. Experimental points are collisional line widths (γ_L) obtained as described above from the fit of function (2) to observed line profiles. Lines in Fig.5 are the best fit of experimental points to linear function. High linearity of all dependences and practically zero intercept of the line corresponding to self-broadening (dashed line) demonstrate good quality of obtained data. Lower part of the figure demonstrates deviations of the self-broadening points from linear dependence in expanded scale. Value of statistical errors (one standard deviation of the γ_L parameter obtained from the lineshape fit) are shown by vertical bars.

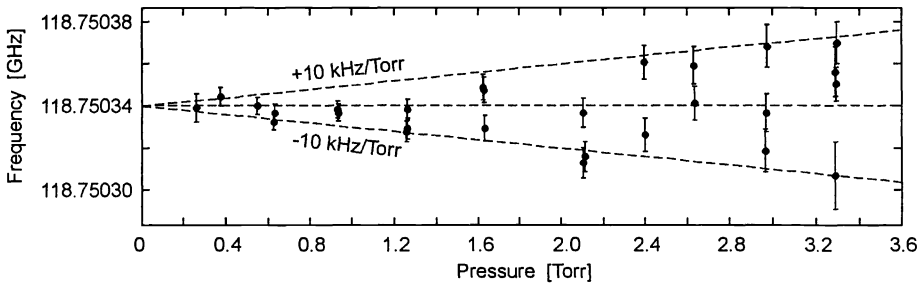

Fig.6. Measured by RAD spectrometer positions of 118 GHz line center frequency vs. pressure.

Positions of 118 GHz oxygen line central frequency (ν_0) also obtained from the fit are plotted vs. pressure in Fig. 6. Random deviations of experimental points from theoretical linear dependence demonstrate that systematic errors are minimized. Studies of such experimental dependences allow accurate determining the line pressure shift parameter (0±10 kHz/Torr in this particular case as a most rigorous estimation) as well as non-shifted center frequency at zero pressure.

The sample pressure range of the spectrometer is from 0.1 – 0.5 Torr up to 5 – 10 Torr depending on studied line broadening and intensity. At lower pressures the acoustic cell becomes deaf (not enough carrier for propagation of acoustic signal). At higher pressures the remaining baseline problems considerably complicates the spectral studies.

The spectrometer can be used in whole range of existing BWOs from long millimeter wave range up to above Terahertz. One of the recent examples is the study of oxygen spectrum from 60 GHz up to 1.2 THz [22, 23]. Frequencies and pressure broadening parameters of all rotational lines and some of lines of the fine structure 60-GHz cluster were measured. The results are presented in Table 1. A few kilohertz for most lines difference between observed and calculated central frequencies well corresponds to classical accuracy limit – linewidth to S/N ratio. This indicates that systematical errors are minimized in these measurements. Examples of observed oxygen spectral lines at 61.8 GHz and at 1120 GHz are shown in Figs. 4B and 4C together with result of fitting of the model function (2) with Lorentz model to the records.

Table 1. Experimental line frequencies and broadening parameters for $^{16}O_2$ ($X^3\Sigma_g^-$, v=0) rotational transitions.

Transition N', J' – N, J	Observed Frequency (MHz)	Frequency Obs.–Calc. (kHz)	Broadening parameters by O_2 (MHz/Torr)	Broadening parameters by N_2 (MHz/Torr)
1, 1 – 1, 2	56 264.785 ± 0.040	+ 8.8	2.21 ± 0.04 (24°C)	2.27 ± 0.01 (24°C)
15, 15–15, 14	56 363.391 ± 0.007	+ 1.5	1.695 ± 0.02 (24°C)	1.580 ± 0.040 (24°C)
5, 5 –5, 4	60 306.052 ± 0.008	– 4.5	1.90 ± 0.02 (24°C)	1.910 ± 0.025 (24°C)
7, 7 –7, 8	60 434.777 ± 0.008	– 2.3	1.81 ± 0.15 (24°C)	1.800 ± 0.025 (24°C)
11, 11–11, 12	61 800.157 ± 0.007	– 0.65	1.735 ± 0.01 (24°C)	1.650 ± 0.03 (24°C)
1, 1 – 1, 0	118 750.340 ± 0.007	+ 2.0	2.23 ± 0.01 (24°C)	2.245 ± 0.02 (24°C)
3, 2 – 1, 1	368 498.245 ± 0.02	– 2.5	2.21 ± 0.03 (31°C)	—
3, 2 – 1, 2	424 763.023 ± 0.02	– 0.9	2.19 ± 0.01 (23°C)	2.215 ± 0.02 (23°C)
3, 3 – 1, 2	487 249.270 ± 0.03	– 8.2	2.10 ± 0.03 (24°C)	2.16 ± 0.1 (26°C)
5, 4 – 3, 3	715 392.980 ± 0.07	+ 67.4	2.08 ± 0.1 (27°C)	—
5, 4 – 3, 4	773 839.510 ± 0.06	+ 6.8	2.01 ± 0.06 (26.5°C)	2.2 ± 0.18 (26.5°C)
5, 5 – 3, 4	834 145.560 ± 0.05	+ 0.3	1.94 ± 0.07 (28°C)	1.96 ± 0.15 (28.5°C)
7, 6 – 5, 5	1 061 123.857 ± 0.1	– 3.6	1.94 ± 0.12 (29.5°C)	—
7, 6 – 5, 6	1 120 714.836 ± 0.04	– 9.4	1.94 ± 0.06 (28.5°C)	1.98 ± 0.15 (29°C)

3.2 Line-shape spectroscopy with resonator spectrometer

The capabilities of RAD spectrometer operating with gases at relatively low pressures are complemented by resonator spectrometer where spectral lines are detected through variation of width of "probe resonance" over the line profile. The measurement of radiation absorption by gas sample in the resonator spectrometer is made through a measurement of the quality factor (Q) of the resonator, which directly depends on the sample absorption value. Q-factor is measured by measurement of width of resonance response. It can be shown (see e.g. [20]) that the sample absorption $\alpha(\nu)$ can be expressed through the resonance width of the resonator using an equation:

$$1 - e^{-\alpha(\nu)\cdot L} = (2\pi \cdot L/c)\cdot(\Delta f(\nu) - \Delta f_0(\nu)), \text{ or } \alpha(\nu) = (2\pi/c)\cdot(\Delta f(\nu) - \Delta f_0(\nu)) \text{ for } \alpha(\nu)\cdot L << 1,$$

where Δf and Δf_0 are respectively widths (FWHM) of the Fabry-Perot resonance with and without sample (or filled by non-absorbing substance), directly measured in the experiment, c – speed of light and L – the resonator length. Typical value of parameters: L = 30 – 40 cm; $Q \sim 600000$; $\Delta f \sim$ 100 – 200 kHz.

Due to indirect measurement of spectral line intensity, the resonator spectrometer do not have problems associated in RAD spectrometer with frequency dependence of incident power $I_0(\nu)$, which limit the range of maximum working pressures of a gas sample to ~10 Torr. Use of the resonator spectrometer allows study of molecular lines in gases at pressures up to one atmosphere and higher. Block-diagram of the spectrometer in given in Fig. 7. The spectrometer employs phase-locked BWO as a broadband radiation source and Fabry-Perot resonator having quality factor near 10^6. The resonance curve of the resonator is recorded in the spectrometer during fast digital frequency scan, and then its shape is fitted to theoretical (Lorentz) profile. The width of resonance is obtained from the fit and used then for calculation of absorption in the sample. Thus the resonance with measurement is made by analogy with measurement of narrow spectral line width, so all factors listed in the section 2.3 should be carefully taken into consideration. Facilitating factor is quite narrow frequency range ($10\Delta f \sim$ 1 MHz) to consider the baseline. Recent introduction of really fast (60 μs/step, switching time 0.2 μs) digital frequency scanning in phase-locked regime without phase jumps while frequency switching [4] for the spectrometer radiation source allowed to achieve for the first time a resonance width

measurement accuracy of ~20 Hz. It corresponds to a radiation absorption coefficient variation sensitivity limit of the spectrometer of ~$4 \cdot 10^{-9}$cm^{-1} or ~0.002 dB/km which exceeds parameters of other previously known analogs in more than order of magnitude.

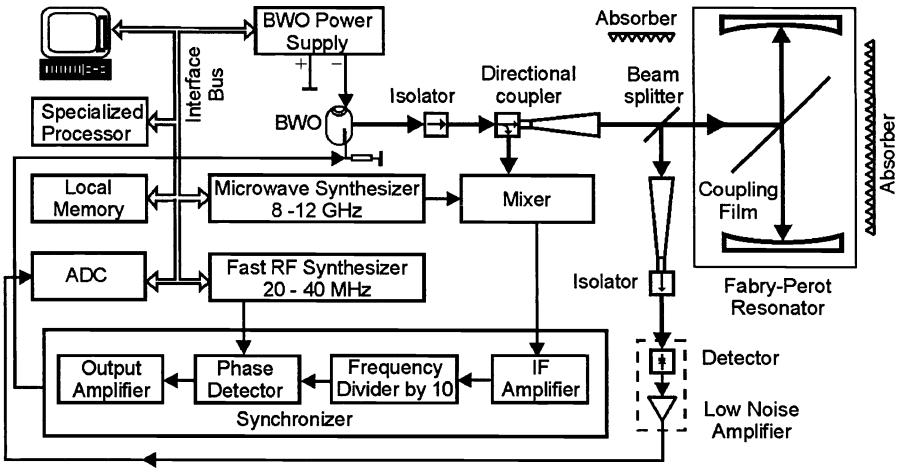

Fig. 7. Block-diagram of the resonator spectrometer with fast frequency scanning.

Fig. 8 (left) presents an example of record of 183-GHz water line in air under atmospheric pressure, room temperature and different air humidity obtained by use of the resonator spectrometer. The line shape fitting function for the resonator spectrometer signal $S_{RS}(\nu)$ should be written as:

$$S_{RS}(\nu) = A_0 F(\nu) + A_1 + A_2(\nu - \nu_0) + A_3(\nu - \nu_0)^2, \quad (3)$$

The second-degree polynomial term is added to take into account a far wings of other atmospheric lines and other non-resonance atmospheric absorption in this frequency range as well as all factors related to residual effects of drifts of the spectrometer parameters during experiments. The multiplicative frequency dependent term is absent due to the spectrometer principle of operation. The Van Vleck-Weisskopf model and accounting the linear dependence on frequency of the integral line intensity were sufficient enough to fit the experimental data to the experimental noise level.

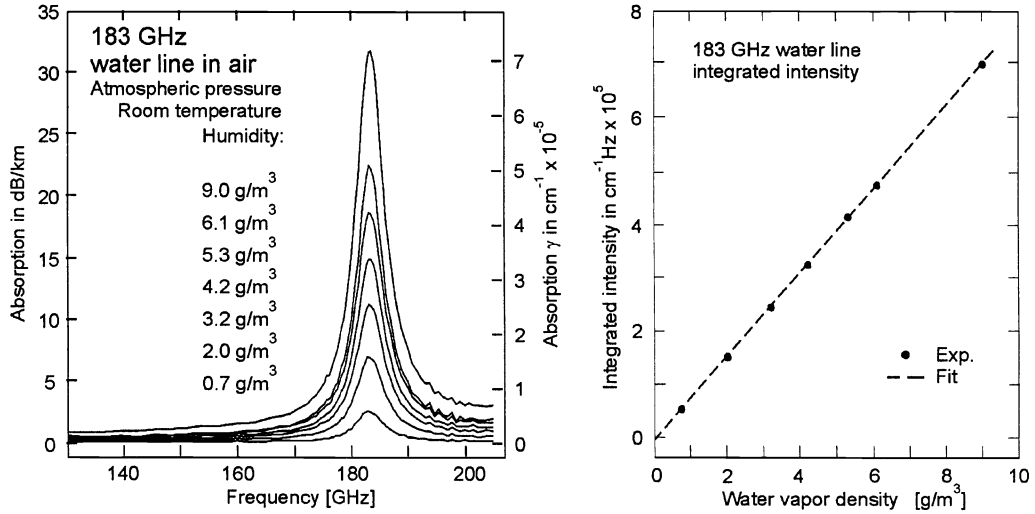

Fig. 8. Water line in air at atmospheric pressure, room temperature and various humidity recorded by use of resonator spectrometer (on the left) and integrated intensity of the line measured using these records (on the right). Dashed line is a best fit of linear function to the experimental points.

To demonstrate high accuracy of spectral line parameters obtained by such way integrated line intensities were calculated for each experiment as the observed line amplitude (the line absorption coefficient at the line central frequency) multiplied by the pi times line half width ($\pi \cdot \alpha(\nu_0) \cdot \gamma_L$) and plotted vs. the sample absolute humidity. The result is presented in Fig. 8 (right) together with a best fit of the points to linear function. The experimental points confirm very well the linear going to zero theoretical dependence. The line intensity (α_{line}) value calculated from these experimental data for constitutes $0.780(8)\times10^{-22}$ cm/molecule, what coincides with the calculated value given is spectroscopic databases GEISA and HITRAN within 0.4%. It should be also pointed out that the resonator spectrometer experiment confirmed the presence of the line center frequency pressure shift and determined the value (– 53 MHz) of the shift in air at atmospheric pressure, which was noticed for a first time from the Earth atmosphere limb sounding data fitting results [19]. With more details the water line study is described in [20].

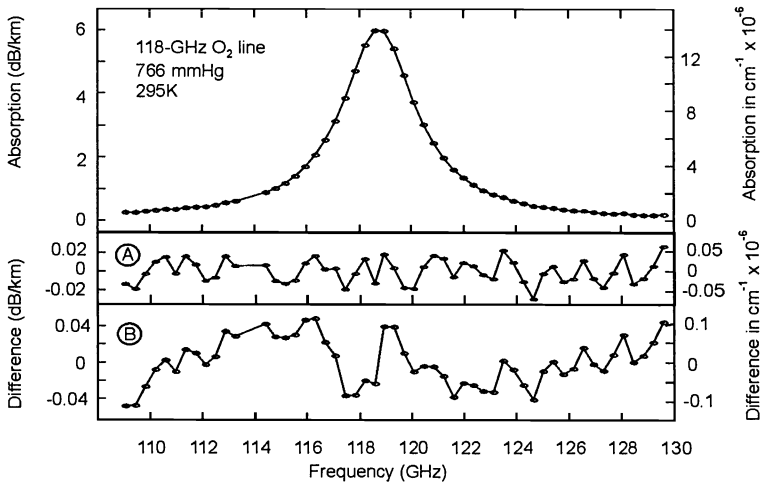

Fig. 9. Resonator spectrometer records of the 118-GHz oxygen line (upper part) in pure oxygen (circles) at pressure 766 Torr, temperature 22°C, and best fit of model function to the experiment (solid curve). In lower part there are expanded residuals of the fit (*A*) Rosenkranz model [10] and (*B*) Van Vleck-Weisskopf model.

Another recent example of a true line shape spectroscopy with the resonator spectrometer use is the first laboratory measurement of the mixing coefficients for the 118-GHz oxygen line [24]. Experimental records of the line with S/N ratio of about 400 (Fig. 9) demonstrated clear deviations from the Van Vleck-Weisskopf model but allowed fitting to the experimental noise level if the Rosenkranz lineshape model [10] was used in the fitting function (3) with the line mixing coefficient as adjustable parameter. It should be also mentioned that the use of Van Vleck-Weisskopf model lead to determination of the line central frequency shifted down relatively the line center measured at low pressure at about 50 MHz. If the experimental S/N ratio would be just a few times less then the Van Vleck Weisskopf model could seem to be adequate and the shift could appear as common linear with pressure shift. Whereas the use of the Rosenkranz model allowed to measure the line mixing coefficient and confirmed the results obtained by use of RAD spectrometer (Fig. 6) that the linear with pressure shift of the line can not exceed ±10 kHz/Torr. The measured mixing coefficient –4.62(38) $Torr^{-1}$ differs by about 50% from previously used calculated value. The line broadening parameters by pressure of pure oxygen and dry air obtained from the resonator spectrometer experiments as 2.24(1) MHz/Torr and 2.25(3) MHz/Torr correspondingly [24] coincided with value of these parameters obtained from RAD experiment (see Fig. 5 and Table 1 above) within 0.5%, although the average sample pressures in two experiments differ more than 300 times. Such a good coincidence proofs that the systematical errors of the line parameters measurements are minimized in both spectrometers.

ACKNOWLEDGEMENTS

Author is grateful to A.F. Krupnov and G.Yu. Golubiatnikov for reading the manuscript and for their valuable comments. Studies described in this work were supported in parts by Russian Foundation for Basic Research and by Ministry of Industry, Science and Technology.

REFERENCES

1. J. Urban, *J. Quant. Spectrosc. Radiat. Transfer* **76** (2003) 145-178.
2. C.A. Gottlieb, P.C. Myer, P. Thaddeus, *Proceedings of the 58th International Symposium on Molecular Spectroscopy.* Ohio State University, USA, June 16-20 (2003) RE07.
3. A.F. Krupnov, in: G.W. Chantry, (Ed.), *Modern Aspects of Microwave Spectroscopy.* Academic Press, L, (1979) pp. 217 – 256. V.N. Markov, G.Yu. Golubiatnikov et al. *J. Mol. Spectrosc.* **212** (2002) 1-5.
4. A.F. Krupnov, M.Yu. Tretyakov, V.V. Parshin, V.N. Shanin, S.E. Myasnikova, *J. Mol. Spectrosc.* 202 (2000) 107 - 115.
5. C. Puzzarini, L. Dore, G. Cazzoli, *J. Mol. Spectrosc.* 216 (2002) 428 - 436.
6. S.G. Rautian, I.I. Sobel'man, *Sov. Phys.Usp.* Engl. Transl. 9 (1967) 701-716.
7. L. Galatry, *Phys. Rev.* 122 (1960) 1218-1224.
8. T.Kohler, H. Mader, Mol. Phys. 86 (1995) 287-300.
9. I. Morino, K.M.T. Yamada, *J. Mol. Spectrosc.* 219 (2003) 282-289.
10. P.W. Rosenkranz, *J. Quant. Spectrosc. Radiat. Transfer.* 39 (1988) 287-297.
11. J. R. Rusk, *J. Chem. Phys.* **42,** 493–500 (1965).
12. Yu. A. Dryagin, A. G. Kislyakov, L. M. Kukin, A. I. Naumov, and L. I. Fedoseev, *Izv. VUZov, Radiofizika* **9,** 1078–1084 (1966). [in Russian; available in English as *Radiophysics and Electronics*]
13. L. Frenkel and D. Woods, *Proc. IEEE* **54,** 498–505 (1966).
14. C.O. Hemmi and A.W. Straiton, *Radio Sci.*, **4**, 9 (1969).
15. V. Ya. Ryadov and N. I. Furashov, *Izv. VUZov, Radiofizika* **18,** 358–369 (1975). [in Russian; available in English as *Radiophysics and Electronics*]
16. A. Bauer, M. Godon, and B. Duterage, *J. Quant. Spectrosc. Radiat. Transfer* **33,** 167–175 (1985)
17. A. Bauer, M. Gordon, M. Kheddar, J.M. Hartmann, *J. Quant. Spectrosc. Radiat. Transfer.* 41 (1989) 49-54.
18. T.M. Goyette, F.C. De Lucia *J. Mol. Spectrosc.* 143 (1990) 346-358.
19. H.C. Pumphrey, S. Buehler, *J. Quant. Spectr. Radiat. Transfer.* 64 (2000) 421 – 437.
20. M.Yu. Tretyakov, V.V. Parshin, M.A. Koshelev, V.N. Shanin, S.E. Myasnikova, A.F. Krupnov, *J. Mol. Spectrosc.* 218 (2003) 239-245.
21. R.A. Toth, L.R. Brown, *J. Mol. Spectrosc.* 218 (2003) 135-150.
22. G.Yu. Golubiatnikov, M.A. Koshelev, A.F. Krupnov, *J. Mol. Spectrosc.* (2003) in press.
23. G.Yu. Golubiatnikov, A.F. Krupnov, *J. Mol. Spectrosc.* 217 (2003) 282-287.
24. M.Yu. Tretyakov, G.Yu. Golubiatnikov, V.V. Parshin, M.A. Koshelev, S.E. Myasnikova, A.F. Krupnov, and P.W. Rosenkranz. *J. Mol. Spectrosc.* (2003) in press.